AS 712 Project

William J. Longley

1 Introduction

Incoherent scatter radars (ISR) measure the power returned by radar pulses that are Thomson scattered off electrons in the ionosphere. The measured spectrum can then be inverted to calculate the local electron density, electron temperature, ion temperature, and bulk plasma flow speed [*Milla and Kudeki*, 2006; *Hysell et al.*, 2015]. The measured spectra also depends heavily on the magnetic aspect angle, which is defined as 0° when viewing perpendicular to the magnetic field. For aspect angles greater than 5°, the plasma is effectively collisionless, and the theoretical spectra has been worked out in detail by *Kudeki and Milla* [2011]. Figure 1 shows this theoretical spectra at a magnetic aspect angle of 90°.

At magnetic aspect angles less than 5°, the effects of Coulomb collisions become important, and the returned spectra is narrower than expected [*Sultzer and Gonzalez*, 1999; *Milla and Kudeki*, 2011]. Sultzer and Gonzalez argue that at small aspect angles the radar does not see the motion of electrons along the magnetic field line, and thus the changes in motion due to Coulomb collisions become the dominant method for affecting the phase of the radar signal. My current research is to add Coulomb collisions to a Particle-in-Cell (PIC) simulator, and use that code to simulate ISR spectra at small magnetic aspect angles. This paper will cover the radiative transfer theory involved in ISR, and will lay the groundwork for correctly obtaining ISR spectra from the collisional PIC code.

2 ISR Theory

The radar pulses transmitted into the ionosphere are linearly polarized. The electric field transmitted by the radar can then be written as

$$\vec{\boldsymbol{E}}(x) = E_0 \, Re[e^{ik_0 x}]\hat{\boldsymbol{z}} \qquad \textit{Eq. 1}$$

Where we have chosen coordinates such that the electric field is polarized in the z-direction, and the wave is propagating in the negative x-direction. This electric field will cause electrons to oscillate sinusoidally in the z-direction as the wave passes through mostly unimpeded. However, ISR transmitters operate on Giga-Watt power scales, so enough photons are transmitted that some will scatter off the oscillating electrons. Since the electron is oscillating at a frequency $\omega_0 = ck_0$, any photons that do scatter off the electron will do so through Thomson scattering. Equations 3.34 and 3.24 in *Rybicki and Lightman* [1979] provide the expressions for the dipole moment and dipole radiation pattern for an oscillating electron under Thomson scattering:

$$\ddot{\boldsymbol{d}} = \frac{e^2 E_i}{m_e} Re[e^{i\omega_0 t}]\,\hat{\boldsymbol{z}} \qquad \textit{Eq. 2}$$

$$\vec{\boldsymbol{E}}(t) = \ddot{\boldsymbol{d}}(t)\frac{\sin\Theta}{c^2 R_0} \qquad \textit{Eq. 3}$$

Where R_0 is the distance from the electron to the radar receiver. Θ is the angle between the charge's motion, which is in the z-direction, and the receiver's line of sight, which is in the x-direction. We note that $t = R_0/c$, and thus we can combine Equations 2 and 3 to obtain

$$\vec{\boldsymbol{E}}(t) = \frac{e^2 E}{m_e} \frac{Re[e^{i(k_0 c)(R_0/c)}]}{c^2 R_0}\, \hat{\boldsymbol{z}} \qquad \textit{Eq. 4}$$

Equation 1 provides the expression for the electric field, and we substitute that into Equation 4,

$$\vec{\boldsymbol{E}}(t) = \frac{e^2}{m_e} E_0\, Re\left[e^{ik_0 R_0}\right] \frac{Re\left[e^{ik_0 R_0}\right]}{c^2 R_0}\, \hat{\boldsymbol{z}} \qquad \textit{Eq. 5}$$

The exponential terms can be combined, so this equation simplifies to

$$\vec{\boldsymbol{E}}(t) = \frac{e^2 E_0}{c^2 R_0 m_e}\, Re[e^{2ik_0 R_0}]\hat{\boldsymbol{z}} \qquad \textit{Eq. 6}$$

Equation 6 provides the expression for the scattered electric field that the radar receiver will measure. One thing to note is that Equation 6 is a sine wave with a wavelength that is half of the incident wavelength. This is referred to in the ISR community as the Bragg vector, but it does not have any relation to Bragg scattering off of crystals other than the factor of 2. For convenience, we redefine the wave number such that

$$\vec{\boldsymbol{k}} = 2\vec{\boldsymbol{k}}_0 \qquad \textit{Eq. 7}$$

The classical electron radius is defined as $r_e = e^2/m_e c^2$, so we can rewrite Equation 6 as

$$\vec{\boldsymbol{E}}(t) = \frac{r_e}{R_0} E_0\, Re[e^{ikR_0}]\hat{\boldsymbol{z}} \qquad \textit{Eq. 8}$$

Equation 8 is the expression for the Thomson scattered electric field off a single electron in the ionosphere, which has an effective collision cross section of

$$\sigma = \frac{8\pi}{3}\, R_0^2 \qquad \textit{Eq. 9}$$

If N_e is the average number density of the electrons in the ionosphere, then a large volume V of the plasma will contain N_eV electrons. Since electromagnetic fields obey the superposition principle, the total electric field scattered off the volume and measured by the radar receiver is then

$$\vec{\boldsymbol{E}}_{tot}(t) = E_0 r_e \sum_{j=1}^{N_e V} \frac{1}{R_{0,j}}\, Re\left[e^{ikR_{0,j}}\right] \hat{\boldsymbol{z}} \qquad \textit{Eq. 10}$$

The ionosphere starts at about 100 km in altitude, and the beam width of the radar is less than 1°, so we can make the approximation that $\vec{\boldsymbol{R}}_{\boldsymbol{0,j}} \cong \vec{\boldsymbol{R}}_{\boldsymbol{0}}$. Thus we have

$$\vec{\boldsymbol{E}}_{tot}(t) = \frac{E_0 r_e}{R_0} \sum_{j=1}^{N_e V} Re\left[e^{ikR_{0,j}}\right] \hat{\boldsymbol{z}} \qquad \textit{Eq. 11}$$

The particle positions in the exponential cannot be approximated as R_0 though, since the resulting phase of $\boldsymbol{E}_{tot}$ is highly sensitive to the value of the exponential for each particle.

Equation 11 calculates the total electric field returned to the radar after Thomson scattering off of bulk electrons. From Parseval's theorem and Equation 2.33 in *Rybicki and Lightman* [1979], the spectrum measured by the radar is

$$\frac{dW}{dA\, d\omega} = c\left|\vec{\boldsymbol{E}}(\omega)\right|^2 \qquad \textit{Eq. 12}$$

Where $\vec{\boldsymbol{E}}(\omega)$ is the time Fourier transform of Equation 11.

3 ISR Simulations

To simulate the spectra an ISR site will measure we use a particle-in-cell (PIC) code that treats ions and electrons as individual particles in a spatial domain. At each time step, the charge density is calculated using the particle positions. With the charge density, Poisson's equation can be numerically integrated to find the electric field at all points in the domain. Knowing the electric field, an externally imposing a static magnetic field, the Lorentz force on each particle is computed and a standard leap-frog scheme updates the position and velocity of every particle.

Because PIC schemes must calculate charge density to invert Poisson's equation at every time step, the particle density of every species is also calculated and output at each time step. Rearranging Equation 11 will show how we can simulate the ISR spectra by knowing the density outputs. First, we note that the density for discrete electrons in a volume *V* can be written as

$$n_e(\vec{\boldsymbol{x}}, t) = \sum_{j=1}^{j=N_e V} \delta(\vec{\boldsymbol{x}} - \vec{\boldsymbol{r}}_{\boldsymbol{j}}(t)) \qquad \textit{Eq. 13}$$

Where N_e is the average electron density, in comparison to the locally varying electron density n_e. Fourier transforming n_e in all three spatial dimensions yields

$$n_e\left(\vec{\boldsymbol{k}}, t\right) = \int_{-\infty}^{\infty} n_e(\vec{\boldsymbol{x}}, t)\, e^{i\vec{\boldsymbol{k}}\cdot\vec{\boldsymbol{x}}} d\vec{\boldsymbol{x}} \qquad \textit{Eq. 14}$$

$$n_e\left(\vec{\boldsymbol{k}}, t\right) = \int_{-\infty}^{\infty} \left[\sum_{j=1}^{j=N_e V} \delta\left(\vec{\boldsymbol{x}} - \vec{\boldsymbol{r}}_{\boldsymbol{j}}(t)\right) \right] e^{i\vec{\boldsymbol{k}}\cdot\vec{\boldsymbol{x}}} d\vec{\boldsymbol{x}} \qquad \textit{Eq. 15}$$

The integration in Equation 15 is over a summation of Dirac delta distributions, so the integral is easily simplified to

$$n_e\left(\vec{\boldsymbol{k}}, t\right) = \sum_{j=1}^{j=N_e V} e^{i\vec{\boldsymbol{k}}\cdot\vec{\boldsymbol{r}}_j} \qquad \textit{Eq. 16}$$

This is the quantity present in Equation 11, though Equation 16 is generalized to wavenumbers that are not necessarily directed along $\vec{\boldsymbol{r}}_{\boldsymbol{j}} \equiv \vec{\boldsymbol{R}}_{0,j}$ Substituting Equation 16 into Equation 11 yields

$$\vec{\boldsymbol{E}}_{tot}(t) = \frac{E_0 r_e}{R_0}\, Re\left[n_e\left(\vec{\boldsymbol{k}}, t\right)\right] \hat{\boldsymbol{z}} \qquad \textit{Eq. 17}$$

We can now Fourier transform Equation 17 to obtain $\vec{\boldsymbol{E}}(\omega)$ in order to find the spectra.

$$\vec{\boldsymbol{E}}(\omega) = \frac{E_0 r_e}{R_0} \int_{-\infty}^{\infty} n_e(\vec{\boldsymbol{k}}, t)\, e^{i\omega t}\, dt\, \hat{\boldsymbol{z}} \qquad \textit{Eq. 18}$$

This integration is the time Fourier transform of n_e, where we define the forward transform without the 2π normalization. Additionally, we do not take the real part of $\boldsymbol{n_e}(\vec{\boldsymbol{k}}, \boldsymbol{t})$ since we are now calculating $n_e(\vec{\boldsymbol{k}}, \omega)$, which should be done as four consecutive Fourier transforms of $n_e(\vec{\boldsymbol{r}}, t)$. Thus we obtain

$$\vec{\boldsymbol{E}}(\omega) = \frac{E_0 r_e}{R_0}\, n_e(\vec{\boldsymbol{k}}, \omega)\, \hat{\boldsymbol{z}} \qquad \textit{Eq. 19}$$

$$\left|\vec{\boldsymbol{E}}(\omega)\right|^2 = \frac{E_0^2 r_e^2}{R_0^2} \left|n_e(\vec{\boldsymbol{k}}, \omega)\right|^2 \qquad \textit{Eq. 20}$$

Finally, substituting this into Equation 12 produces the spectra as a function of a quantity we can simulate in PIC codes: electron density.

$$\frac{dW}{dA\, d\omega} = c \frac{E_0^2 r_e^2}{R_0^2} \left|n_e(\vec{\boldsymbol{k}}, \omega)\right|^2 \qquad \textit{Eq. 21}$$

4 Conclusions

In this paper we used the fundamentals of radio waves Thomson scattering off a large group of electrons in the ionosphere in order to arrive at Equation 21. This equation relates the small scale plasma kinetic processes in a PIC code to the observed spectra obtained by bouncing a powerful radio signal off the ionosphere. Figure 1 shows the results of a PIC simulation, which is produced by taking 96 independent averages of Equation 21 in order to smooth out the simulation noise. This averaging is analogous to the ISR sites integrating the measured spectra over a set time.

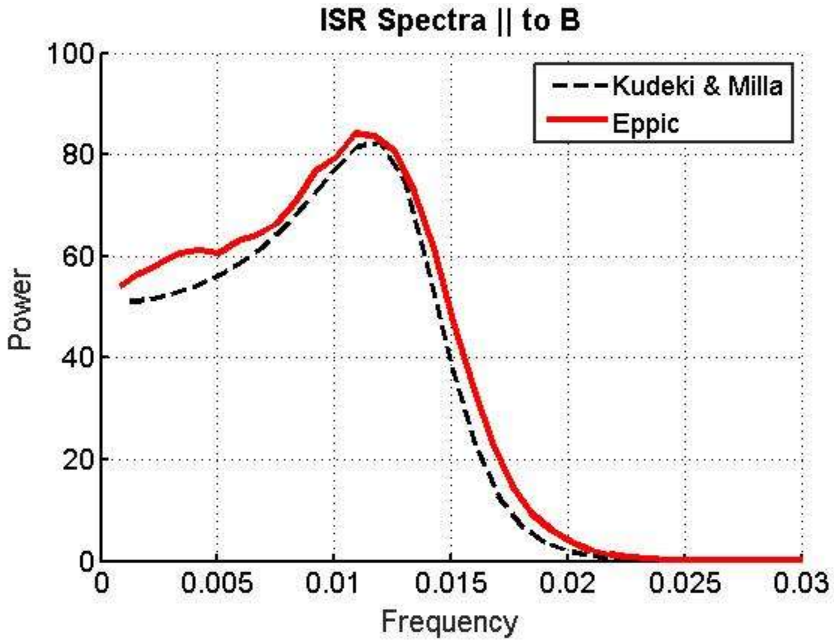

Figure 1. Theoretical and particle-in-cell simulated ISR spectra taken parallel to the magnetic field, which is a magnetic aspect angle of 90°. The frequencies are normalized to the electron

plasma frequency. The size of the “double hump” feature is related to the electron-ion temperature ratio, which is 2 in this plot. The width of the spectra is determined by the ion temperature, and the power returned is proportional to the electron density. The bulk movement of the plasma can be calculated if the spectra is Doppler shifted. The theoretical plot is generated using the results from *Kudeki and Milla* [2011].

References

Hysell, D. L., M. A. Milla, F. S. Rodrigues, R. H. Varney, and J. D. Huba (2015), Topside equatorial ionospheric density, temperature, and composition under equinox, low solar flux conditions. J. Geophys. Res. Space Physics, 120, 3899–3912. doi: 10.1002/2015JA021168.

Kudeki, E., and M. Milla (2011), Incoherent scatter spectral theories part I: A general framework and results for small magnetic aspect angles. IEEE Trans. Geosci. Remote Sens., 49(1), 315–328. doi: 10.1109/TGRS.2010.2057252

Milla, M., and E. Kudeki (2006), F-region electron density and Te/Ti measurements using incoherent scatter power data collected at ALTAIR. Ann. Geophys., 24, 1333–1343. doi: 10.5194/angeo-24-1333-2006

Milla, M., and E. Kudeki (2011), Incoherent scatter spectral theories part II: Modeling the spectrum for modes propagating perpendicular to B. IEEE Trans. Geosci. Remote Sens., 49(1), 329–345. doi: 10.1109/TGRS.2010.2057253

Oppenheim, M. M., Y. S. Dimant, and L. P. Dyrud (2008), Large-scale simulations of 2D fully kinetic Farley-Buneman turbulence. Ann Geophy., 26, 453-553. doi: 10.5194/angeo-26-543-2008

Rosenbluth, M. N., W. M. MacDonald, and D. L. Judd (1957), Fokker-Planck equation for an inverse square force. Phys. Rev., Vol 107, No 1. doi: 10.1103/PhysRev.107.1

Rybicki, G. B. and A. P. Lightman (1979), Radiative Processes in Astrophysics. Wiley-VCH.